Phytochemistry 215 (2023) 113853

Contents lists available at ScienceDirect

Phytochemistry

journal homepage: www.elsevier.com/locate/phytochem

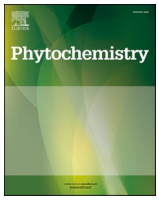

Cytotoxic triterpenoid saponins from the root of Olax subscorpioidea Oliv. (Olacaceae)

Yemi A. Adekunle [a,c,d,*], Babatunde B. Samuel [a,**], Lutfun Nahar [b,***], Amos A. Fatokun [c], Satyajit D. Sarker [c]

[a] Department of Pharmaceutical Chemistry, Faculty of Pharmacy, University of Ibadan, Nigeria
[b] Laboratory of Growth Regulators, Palacký University and Institute of Experimental Botany, The Czech Academy of Sciences, Šlechtitelů 27, 78371, Olomouc, Czech Republic
[c] Centre for Natural Products Discovery, School of Pharmacy and Biomolecular Sciences, Faculty of Science, Liverpool John Moores University, Byrom Street, L3 3AF, Liverpool, United Kingdom
[d] Department of Pharmaceutical and Medicinal Chemistry, College of Pharmacy, Afe Babalola University, Ado-Ekiti, Nigeria

ARTICLE INFO

Keywords:
Olax subscorpioidea, Olacaceae
Cancer
Triterpene saponins

ABSTRACT

Bioactivity-guided phytochemical fractionation of the methanol extract of *Olax subscorpioidea* root has led to the isolation of six triterpenes. Three of these compounds are previously undescribed triterpenoid saponins: oleanolic acid 3-*O*-[*α*-L-rhamnopyranosyl-(1→3)-*β*-D-glucopyranosyl-(1 → 2)-6-*O*-methyl-*β*-D-glucuronopyranoside]-28-*O*-*β*-D-glucopyranosyl ester (**2**), oleanolic acid 3-*O*-[*β*-D-glucopyranosyl-(1 → 4)-*β*-D-glucopyranosyl-(1 → 3)-*β*-D-glucopyranoside] (**3**), and oleanolic acid 3-*O*-[*β*-D-glucopyranosyl-(1 → 4)-6-*O*-methyl-*β*-D-glucuronopyranoside] ester (**5**). Other reported known compounds include two triterpene glycosides: oleanolic acid 3-*O*-[*β*-D-glucopyranosyl-(1 → 4)-6-*O*-methyl-*β*-D-glucuronopyranoside]-28-*O*-*β*-D-glucopyranosyl ester **(1)** and oleanolic acid 3-*O*-[*β*-D-glucopyranosyl-(1 → 4)-*β*-D-glucuronopyranoside] **(4)**; and a triterpene acid, oleanolic acid **(6)**. The structures of these compounds were elucidated by spectroscopic means. The isolated compounds were tested against human cervical cancer (HeLa), colorectal cancer (Caco-2) and breast cancer (MCF-7) cell lines using the *in vitro* 3-[4,5-dimethylthiazole-2-yl] 3,5-diphenyltetrazolium bromide (MTT) assay, with vincristine as positive control. The cytotoxicity assay showed that compounds **3** and **5** exhibited significant inhibitory effects on the HeLa cell line, with IC_{50} values of 7.42 ± 0.34 μM and 10.27 ± 1.26 μM; and moderate effects on MCF-7 (IC_{50} values, 36.67 ± 1.23 μM and 43.83 ± 0.65 μM) and Caco-2 (IC_{50} values, 35.83 ± 0.55 μM and 39.03 ± 4.38 μM, respectively) cell lines. They were also more selectively cytotoxic than vincristine against the cancer cell lines, when compared with cytotoxicity against the normal lung cell line MRC5.

1. Introduction

Cancer continues to be a leading cause of death globally, only second to cardiovascular diseases (CVDs) in mortality rate (Sung et al., 2021). Cancer killed almost 10 million people worldwide with an estimated 19.3 million new cases in 2020 (Ferlay et al., 2021). A recent study has found the rate of CVDs to have reduced during the past decade while cancer, with dangerously rising projections that may overtake CVDs soon, was noted to have an increasing rate (ReFaey et al., 2021). About 70% of all cancer-related deaths are from low- and middle-income countries (Kuete and Efferth, 2015). The global economic cost of cancer has been estimated to be US $1.16 trillion (Stewart and Wild, 2014). Most available anti-cancer drugs are often plagued with severe side effects (Gyanani et al., 2021). There is therefore need for more tolerable, potent, and less toxic anticancer agents. In Africa, medicinal plants remain the most affordable, available, and productive source of anticancer agents; yet they are enormously under-studied (Kuete and Efferth, 2015).

The genus *Olax* L. comprises ethnobotanically important plants indicated in the management of several ailments (Odoma et al., 2020).

* Corresponding author. Department of Pharmaceutical Chemistry, Faculty of Pharmacy, University of Ibadan, Nigeria.
** Corresponding author.
*** Corresponding author.
E-mail addresses: yemiadekunle03@yahoo.com (Y.A. Adekunle), tundebsamuel@gmail.com (B.B. Samuel), nahar@ueb.cas.cz (L. Nahar).

https://doi.org/10.1016/j.phytochem.2023.113853
Received 2 June 2023; Received in revised form 18 August 2023; Accepted 5 September 2023
Available online 7 September 2023

Olax subscorpioidea Oliv. is a shrubby tree which attains a height of about 10 m (Odoma et al., 2017). The plant is called different names by different groups of people in Nigeria: Ifon (Yoruba), Ukpakon (Esan/Edo), Aziza (Nsukka), Igbulu/Osaja (Igbo) and Ocheja (Igala) (Ukwe et al., 2010). Ethnobotanical information has revealed *O. subscorpioidea* has been used traditionally in the management of cancer (Soladoye et al., 2010; Segun et al., 2018). In an ethnobotanical survey carried out among the people living in Ogun State, Southwestern Nigeria, the root of *O. subscorpioidea* was said to be included in the herbal recipe for the management of breast cancer (Gbadamosi and Erinoso, 2016). Preliminary cytotoxic analysis of the methanol root extract of *O. subscorpioidea* showed antiproliferative activity against human rhabdomyosarcoma (RD) and breast cancer (MCF-7) cell lines (Adekunle et al., 2022a).

Although several scientific reports are available on the numerous pharmacological activities of *O. subscorpioidea* including its anticancer potentials, there is a dearth scarcity of information on isolated cytotoxic compounds from the plant (Agbabiaka and Adebayo, 2021; Ahmad et al., 2021; Adekunle et al., 2022b). Forgacs and Provost (1981) isolated an oleanane-type triterpene glycoside, olaxoside, from the leaves, root, and bark extracts of some *Olax* species including *O. andronensis* Baker, *O. glabriflora* P. Danguy and *O. psittacorum* (Lamk) Vahl. Oleanane triterpene acids and glycosides were reported in several *Olax* plants including *O. obtusifolia* De Wild (Pertuit et al., 2018), *O. mannii* Oliv. (Sule et al., 2011), *O. imbricata* Roxb (Nga Thi et al., 2019).

This paper reports bioactivity-guided isolation and structure elucidation of three previously undescribed triterpene glycosides, two known triterpene glycosides and one known triterpene acid from the methanol

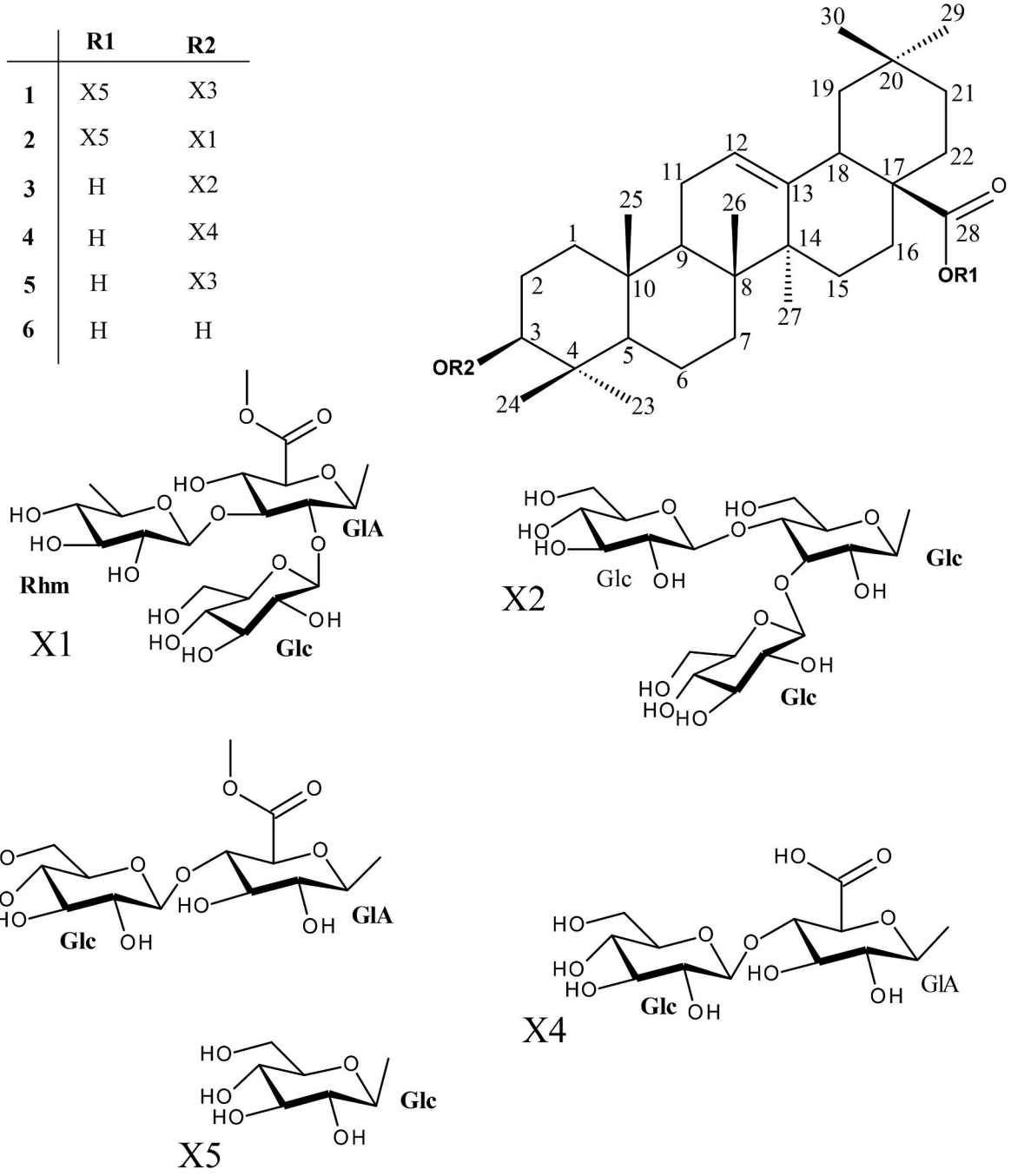

Fig. 1. Chemical structures of compounds **1**–**6** isolated from the root of *O. subscorpioidea*.

root bark extract of *O. subscorpioidea* Oliv. The structures of all compounds were elucidated by spectroscopic means (^{1}H, ^{13}C, DEPT-Q, ^{1}H–^{1}H COSY, ^{1}H–^{13}C HSQC, NOESY, ^{1}H–^{13}C HMBC) together with HR-ESI-MS data and comparing their data with respective literature values. The isolated compounds were tested on three cancer cell lines. The most active compounds were also subjected to selectivity test using MRC5 cell line (Song et al., 2019).

2. Results and discussion

2.1. Structure elucidation

The bioassay-guided separation of the cytotoxic fraction of *O. subscorpioidea* root obtained by Soxhlet extraction (MeOH) led to the isolation of three previously undescribed oleanane-type glycosides (**2, 3** and **5**), two known triterpene glycosides (**1** and **4**), and one triterpene acid (**6**) (Fig. 1). The structures of isolated compounds were determined by extensive spectroscopic experiments, including ^{1}H, ^{13}C-DEPT-Q, ^{1}H–^{1}H COSY, ^{1}H–^{13}C HSQC, NOESY, and ^{1}H–^{13}C HMBC (600 MHz) and HR-ESI-MS, and comparison with the respective literature data. The structure of compound **1** was concluded as oleanolic acid 3-*O*-[*β*-D-glucopyranosyl-(1 → 4)-6-*O*-methyl-*β*-D-glucuronopyranoside]-28-*O*-*β*-D-glucopyranosyl ester (Do et al., 2020), compound **4** was deduced as oleanolic acid 3-*O*-[*β*-D-glucopyranosyl-(1 → 4)-*β*-D-glucuronopyranoside] (Huan et al., 1998; Patkhullaeva et al., 1972; Stefaniak et al., 2018), and compound **6** was concluded as oleanolic acid (Mahato and Kundu, 1994). Compounds **1** and **4** are reported here for the first time in *Olax* genus (Tsakem et al., 2022).

Compound **2** was isolated as a white amorphous powder. Its molecular formula was determined to be $C_{55}H_{88}O_{23}$ from the HR-ESI-MS spectrum which showed an ion peak at *m/z* 1115.5630 $[M-H]^-$ and 1161.5706 $[M + HCOOH]^-$. The IR spectrum showed peaks at 3360 cm^{-1} (OH stretching), 2970 cm^{-1} (CH stretching), 1750 cm^{-1} (C═O stretching), 1690 cm^{-1} (C═O stretching), 1050 cm^{-1} (CO stretching). The 1D NMR data and comparison with the literature data revealed that the aglycone of compound **2** is 3-*β*-hydroxyolean-12-en-28-oic acid (oleanolic acid) (Forgacs and Provost, 1981; Seebacher et al., 2003; Pertuit et al., 2018). The ^{1}H NMR spectrum showed signals assignable to seven angular methyl (-CH_3) groups at δ_H 1.07 (H-23), 0.82 (H-26), 0.97 (H-25), 0.88 (H-24), 1.17 (H-27), 0.93 (H-29) and 0.95 (H-30). The proton NMR spectrum also showed an oxymethine proton at δ_H 3.21 (m, 1H) with HSQC correlation at δ_C 91.1 (C-3). An olefinic proton was determined at δ_H 5.27 (br s, 1H). ^{13}C NMR spectrum showed seven methyl carbon signals for the aglycone at δ_C 27.0 (C-23), 15.5 (C-24), 14.6 (C-25), 16.3 (C-26), 24.9 (C-27), 32.1 (C-29) and 22.6 (C-30) (Table 1). The presence of a methylene group at δ_C 122.4 (C-12)/143.4 (C-13) and of a carbonyl group at δ_C 176.7 were observed.

Previous study had subjected the saponin extract of the root of *O. subscorpioidea* to acid hydrolysis. The acid hydrolysis yielded oleanolic acid, glucose, rhamnose, and xylose (Delaude and Huls, 1982; Pertuit et al., 2018). Biosynthetically, rhamnose synthases use UDP-D-glucose as substrate to form UDP-L-rhamnose, the precursor of L-rhamnose in plant and fungi (Jiang et al., 2021; Gaglianone et al., 2022; Li et al., 2022). Elimination of water occurs between C-5 and C-6 of UDP-D-glucose to form UDP-4-keto-6-deoxy intermediate, which is further acted upon by epimerase-reductase to produce UDP-L-rhamnose (Kamsteeg et al., 1978). In the HSQC spectrum, a methyl doublet at δ_H 1.26 *d* (6.2 Hz, 3H) was observed with a correlation at δ_C 16.4 suggesting the presence of a rhamnose moiety (Gao et al., 2012). The presence of four sugar units in compound **2** was confirmed by their anomeric signals at δ_{HC} 4.60 *d* (8.1 Hz)/103.9, 5.07 *br s*/102.1, 4.62 *d* (7.7 Hz)/102.3, and 5.40 *d* (8.9 Hz)/94.3. For each anomeric proton of a monosaccharide, there are a pair of characteristic chemical shifts and *J* values which are not concentration-dependent (Giner et al., 2016). The chemical shifts and coupling constant of the anomeric proton signal at δ_{HC} 5.07, 1.32 Hz/102.1 agreed with the literature values for *α*-L-rhamnopyranosides (de Bruyn et al., 1976). Consequently, the sugars were identified as glucuronic acid (δ_H 4.60 *d*, 8.1 Hz/103.9), rhamnose (5.07 *br s*/102.1), glucose (4.62 *d*, 7.7 Hz/102.3), and glucose (5.40 *d*, 8.9 Hz/94.3) (Table 2). HMBC experiment suggested that compound **2** was a bisdesmosidic triterpenoid glycoside (Pertuit et al., 2018). HMBC spectrum showed correlations between δ_H 4.60 *d*, 8.1 Hz (GlcA) and δ_C 91.1 (C-3); 4.62 *d*, 7.73 Hz and 76.6 (GlcA-C2′); 5.07 *br s* and 84.3 (GlcA-C3′); and 5.40 *d*, 8.87 Hz and 176.7 (C-28). A methyl ester was noted at δ_H 3.80/δ_C 51.5 which had an HMBC correlation with δ_C 169.6, suggesting a methyl ester of the glucuronic acid (GlcA). The *β*-anomeric configurations of glucuronic acid and glucose units, and *α*-anomeric configuration of rhamnose unit were determined from their $J_{H1,H2}$ coupling constants (7.7–8.5 Hz and 1.3 Hz, respectively) (Zheng et al., 2004). The correlations that were observed between H-3/H-5, H-5/H-9 and H-3/H-1′ in the NOESY spectrum suggested their *α*-axial orientation, hence the *β*-orientation of the oxygen at C-3 and that of glucuronic acid (C1′) (Aliotta et al., 1992; Aouane et al., 2022) (Fig. S13, Supplemental data). Similarly, the coupling constant of rhamnose ($J = 1.3$ Hz) and the axial correlations observed between Rhm-H-1′ at δ_H 5.07/GlA-H-3′ at δ_H 3.70 and GlA-H-3'/GlA-H-1′ at δ_H 4.60 in the NOESY spectrum of **2**, indicated the *α*-configuration of the rhamnose unit. The large coupling constant from the other two anomeric protons ($J = 7.7$ and 8.5 Hz) indicated the *β*-configurations of the glucose units (Liang et al., 2011). Putting the information from COSY, HSQC, NOESY, and HMBC experiments together, and that of HR-ESI-MS spectrum, compound **2** was concluded as oleanolic acid 3-*O*-[*α*-L-rhamnopyranosyl-(1 → 3)-*β*-D-glucopyranosyl-(1 → 2)-6-*O*-methyl-*β*-D-glucuronopyranoside], 28-*O*-*β*-D-glucopyranosyl ester (Fig. 2).

Compound **3** was obtained as a white amorphous powder. Its

Table 1
^{1}H (600 MHz) and^{13}C NMR data (150 MHz) for compounds **2, 3** and **5** in methanol-d_4.

	2		3		5	
	δ_H (*J* in Hz)	δ_C	δ_H (*J* in Hz)	δ_C	δ_H (*J* in Hz)	δ_C
1	1.00[a], 1.65[a]	38.4	0.98[a], 1.61 *m*	38.3	0.92[a], 1.56[a]	38.3
2	1.80[a]	25.6	1.68[a], 1.82 *m*	25.6	1.62[a], 1.73 *m*	25.6
3	3.21 *m*	91.1	3.18 dd (4.6, 11.8)	89.8	3.12 dd (4.3, 12.5)	89.8
4	–	39.0	–	38.8	–	38.8
5	0.79[a]	55.5	0.78[a]	55.6	0.73[a]	55.6
6	1.42[a], 1.56[a]	17.9	1.41[a], 1.56 *m*	17.9	1.36[a], 1.51[a]	17.9
7	1.34[a], 1.50[a]	32.5	1.31[a], 1.53[a]	32.6	1.27[a]	32.6
8	–	39.3	–	39.2	–	39.2
9	1.60 *m*	48.5	1.60 *m*	48.5	1.55 *m*	48.0
10	–	36.5	–	36.5	–	36.5
11	1.90[a]	23.2	1.90 *m*	23.1	1.85[a]	23.1
12	5.27 *br s*	122.4	5.24 *t*	122.3	5.19 *br s*	122.3
13	–	143.4	–	143.8	–	143.8
14	–	41.5	–	41.5	–	41.5
15	1.82[a]	27.5	1.09[a], 1.77[a]	27.4	1.04[a], 1.73 *m*	27.4
16	1.74[a], 2.07[a]	22.6	1.60[a], 2.00 *m*	22.7	1.55[a], 1.96[a]	22.7
17	–	46.6	–	46.2	–	46.3
18	2.87 dd (3.4, 14.2)	41.2	2.85 dd (4.0, 13.8)	41.4	2.80 dd (3.2, 13.7)	41.4
19	1.16[a], 1.74[a]	45.8	1.13[a], 1.69 *t*	45.9	1.08[a], 1.65[a]	45.9
20	–	30.1	–	30.2	–	30.2
21	1.24[a], 1.42[a]	33.5	1.20[a], 1.39[a]	33.5	1.16[a], 1.34[a]	33.5
22	1.63[a], 1.75[a]	31.8	1.54 *m*, 1.74[a]	32.4	1.49[a], 1.70[a]	32.4
23	1.07 *s*	27.0	1.05 *s*	27.1	1.00 *s*	27.1
24	0.88 *s*	15.5	0.84 *s*	15.6	0.80 *s*	15.5
25	0.97 *s*	14.6	0.95 *s*	14.5	0.90 *s*	14.5
26	0.82 *s*	16.3	0.81 *s*	16.3	0.77 *s*	16.3
27	1.17 *s*	24.9	1.16 *s*	25.0	1.12 *s*	25.0
28	–	176.7	–	180.4	–	nd
29	0.93 *s*	32.1	0.91 *s*	32.2	0.86 *s*	32.2
30	0.95 *s*	22.6	0.94 *s*	22.6	0.89 s	22.6

nd: not detected. Assignments were made based on 1D and 2D NMR (^{1}H, ^{13}C, DEPT-Q, COSY, HSQC, NOESY and HMBC) experiments.
[a] Overlapped peaks, confirmed from COSY, HSQC and HMBC correlations.

Table 2
^{1}H (600 MHz) and^{13}C NMR data (150 MHz) of the sugar moieties of compounds **2, 3** and **5** in CD_3OD.

2			3			5		
	δ_H (*J* in Hz)	δ_C		δ_H (*J* in Hz)	δ_C		δ_H (*J* in Hz)	δ_C
3-*O*-GlcA			3-*O*-Glc			3-*O*-GlcA		
1	4.60 *d* (8.1)	103.9	1	4.46 *d* (7.8)	104.9	1	4.38 *d* (8.1)	105.5
2	3.81[a]	76.6	2	3.54 *t*	74.5	2	3.25[a]	73.6
3	3.70[a]	84.3	3	3.93 *t*	80.3	3	3.47 *t*	74.6
4	3.66[a]	70.6	4	4.05[a]	72.9	4	3.69 *t*	80.6
5	3.93[a]	75.2	5	3.67 *m*	70.8	5	3.96 *d* (9.7)	73.6
6	–	169.6	6	3.87 *m*	61.2	6	–	169.5
-CH_3	3.80 *s*	51.5				-CH_3	3.74 s	51.7
3-*O*-Glc			3-*O*-Glc			3-*O*-Glc		
1	4.62 *d* (7.7)	102.3	1	4.56 *d* (7.6)	100.1	1	4.25 *d* (7.7)	103.2
2	3.22[a]	74.2	2	3.32[a]	77.2	2	3.12 *t*	73.3
3	3.38[a]	76.5	3	3.34[a]	76.0	3	3.27 *t*	76.3
4	3.11 *t*	71.0	4	3.33[a]	69.7	4	3.24[a]	70.0
5	3.28[a]	77.3	5	3.31[a]	72.6	5	3.30[a]	76.8
6	3.58[a], 3.86[a]	62.1	6	3.69 *m*, 3.89[a]	61.2	6	3.60 *m*, 3.83[a]	61.1
3-*O*-Rham			3-*O*-Glc					
1	5.07 *br s* (1.3)	102.1	1	4.85[a]	102.9			
2	4.05[a]	70.8	2	3.29[a]	76.9			
3	3.68[a]	70.8	3	3.37[a]	76.4			
4	3.44[a]	72.4	4	3.32[a]	69.9			
5	3.95[a]	69.3	5	3.29[a]	74.0			
6	1.26 *d* (6.2)	16.4	6	3.66 *m*, 3.86[a]	61.2			
28-O-Glc								
1	5.40 *d* (8.5)	94.3						
2	3.34[a]	72.5						
3	3.66[a]	70.6						
4	3.95[a]	69.3						
5	3.44[a]	72.4						
6	3.70[a], 3.82[a]	61.0						

Assignments were made based on 1D and 2D NMR (^{1}H, ^{13}C, DEPT-Q, COSY, HSQC, NOESY and HMBC) experiments.
[a] Overlapped peaks, confirmed from COSY, HSQC and HMBC correlations.

molecular formula was deduced as $C_{48}H_{78}O_{18}$ from its HR-ESI-MS spectrum showing molecular ion peak at *m/z* 942.6393 [M-H]$^-$. The IR spectrum showed peaks at 3300 cm^{-1} (OH stretching), 2930 cm^{-1} (CH stretching), 1750 cm^{-1} (C═O stretching), 1690 cm^{-1} (C═O stretching), 1020 cm^{-1} (CO stretching). ^{1}H NMR spectrum revealed seven (7) angular methyl groups at 1.05 (H-23), 0.95 (H-25), 0.84 (H-24), 1.16 (H-27), 0.94 (H-30), 0.91 (H-29) and 0.81 (H-26). An oxy-methine proton at 3.18 dd (4.6, 11.8 Hz) and an olefinic proton at δ_H 5.24 (t, 1H) were observed. Three anomeric protons at δ_C 4.85, 4.56 (*d*, 7.6 Hz) and 4.46 (*d*, 7.8 Hz) were observed. ^{13}C-DEPT-Q showed peaks for seven (7) tertiary methyl groups at δ_C 32.2 (C-29), 27.1 (C-23), 25.0 (C-27), 22.6 (C-30), 16.3 (C-26), 15.6 (C-24) and 14.5 (C-25) (Table 1). An oxy-methine carbon at δ_C 89.8; two olefinic carbon signals at δ_C 122.3 and 143.8; three anomeric carbons at δ_C 104.9, 102.9 and 100.1; one carbonyl carbon at δ_C 180.4 were also observed. Other sugar peaks occurred between δ_C 61.2–80.3. Compound **3**, like **2**, has an olean-12-en-28-oic acid triterpene skeleton (Mahato and Kundu, 1994). A ^{1}H–^{13}C long-range correlation in the HMBC spectrum existed between the sugar anomerics at δ_H 4.46 and δ_C 89.8 (C-3). Another correlation was observed between the sugar anomeric at δ_H 4.85 and δ_C 80.3 (C3′); and between sugar anomeric δ_H 4.56 and δ_C 72.9 (C4′). The *β*-anomeric configurations of glucose units were determined from their $J_{H1,H2}$ coupling constants (7.6–7.8 Hz) (Zheng et al., 2004). Like compound **2**, correlations were observed between H-3/H-5, and H-3/H-1′ in the NOESY spectrum indicating their *α*-axial orientation, hence the *β*-orientation of the oxygen at C-3 and the glucose at C1′ (Aliotta et al., 1992; Aouane et al., 2022) (Fig. S20, Supplemental data). The large coupling constant from the glucose anomeric protons ($J > 7.7$ Hz) indicated the *β*-configurations of the other glucose units (Liang et al., 2011). Based on extensive NMR and MS experiments, the structure of compound **3** was concluded as oleanolic acid 3-*O*-[*β*-D-glucopyranosyl-(1 → 4)-*β*-D-glucopyranosyl-(1 → 3)-*β*-D-glucopyranoside] (Fig. 2).

Compound **5** was obtained as a white amorphous powder. HR-ESI-MS spectrum showed a molecular ion peak at *m/z* 807.4502 [M-H]$^-$ calculated for $C_{43}H_{68}O_{14}$. The IR spectrum showed signals at 3350 cm^{-1} (OH stretching), 2920 cm^{-1} (CH stretching), 1750 cm^{-1} (C═O stretching), 1695 cm^{-1} (CO stretching), and 1020 cm^{-1} (CO stretching). ^{1}H NMR showed seven (7) angular methyl peaks at δ_H 1.00 (H-23), 0.90 (H-25), 0.86 (H-29), 1.12 (H-27), 0.89 (H-30), 0.80 (H-24) and 0.77 (H-26). An oxy-methine proton at δ_H 3.12 (C-3); an olefinic proton at δ_H 5.19 (br s, 1H, C-12); and two anomeric protons at δ_H 4.38 *d* (8.1 Hz) and 4.25 *d* (7.7 Hz) were observed. ^{13}C-DEPT-Q showed signals for seven methyl functional groups at δ_C 32.2 (C-29), 27.1 (C-23), 25.0 (C-27), 22.6 (C-30), 16.3 (C-26), 15.5 (C-24) and 14.5 (C-25). Two olefinic carbon signals were observed at δ_C 122.3 and 143.8. In addition, two anomeric carbons at δ_C 105.5 and 103.2 were noted. Carbon signals for sugar moieties occurred at δ_C 61.1–80.6 (Tables 1 and 2). No other evidence of glycosylation was noted. The NMR data agreed with that of olean-12-en-28-oic acid triterpenes (Agrawal and Jain, 1992). HMBC showed a long-range connectivity between an anomeric proton at δ_H 4.38 and δ_C 89.8 (C-3). A carbonyl functional absorption at δ_C 169.5 indicated a uronic acid with a long-range HMBC correlation of a methyl group at δ_H 3.74. The anomeric proton (δ_H 4.25) correlated with carbon δ_C 80.6 in the HMBC experiment. The *β*-anomeric configurations of glucuronic acid and glucose units were determined from their $J_{H1,H2}$ coupling constants (7.7–8.1 Hz) (Zheng et al., 2004). The configurations were confirmed from the NOESY experiment in which correlations were observed between H-3/H-5, and H-3/H-1′, indicating their *α*-axial orientation, and thus *β*-orientation of the oxygen at C-3 and glucuronic acid (C1′) (Aliotta et al., 1992; Aouane et al., 2022). The large coupling constant from the anomeric protons ($J = 7.7$ Hz) indicated the *β*-configurations of the glucose unit (Liang et al., 2011) (Fig. S34). Extensive NMR data analysis and comparison with published data led to the conclusion of compound **5** as oleanolic acid 3-*O*-[*β*-D-glucopyranosyl-(1 → 4)-6-*O*-methyl-*β*-D-glucuronopyranoside] (Fig. 2).

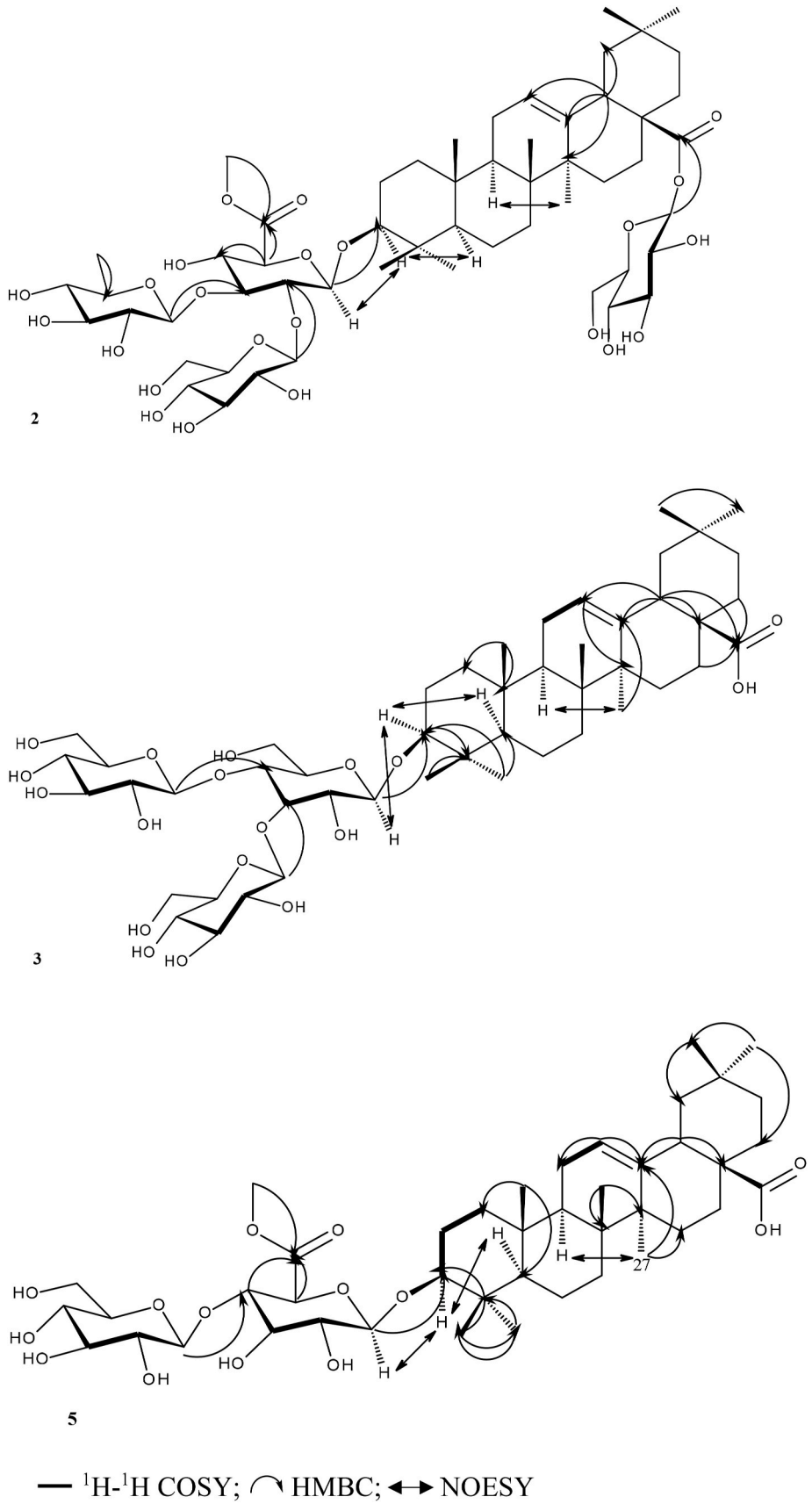

Fig. 2. Key ^{1}H–^{1}H COSY, NOESY, and ^{1}H–^{13}C HMBC correlations of compounds **2, 3** and **5** isolated from the root of *O. subscorpioidea*.

2.2. In vitro cytotoxicity

MTT assay was used to evaluate the cytotoxicity of the isolated compounds **1**–**6** in concentrations that ranged from 12.5 to 200 μM against human breast cancer (MCF-7), cervical cancer (HeLa), and colorectal cancer (Caco-2) cell lines. Vincristine was used as a positive reference drug or positive control. Compounds **3, 4, 5**, and **6** were found to possess cytotoxic activity with IC_{50} values ranging from 7.42 ± 0.34 μM to 110.21 ± 15.64 μM (Tables 3 and 4). Oleanane-type triterpenes have been noted to have evidence of anticancer effects (Parikh et al., 2014). Compound **6**, oleanolic acid, had been reported to possess cytotoxic actions on various cancer cell lines (Feng et al., 2009). The highest activity was observed in compound **3**, a 3-triglucoside derivative of oleanolic acid. Compound **3** displayed strong cytotoxicity on HeLa (IC_{50} value, 7.42 ± 0.34 μM) and moderate activity on MCF-7 (IC_{50}, 36.67 ± 1.23 μM) and Caco-2 (IC_{50}, 35.83 ± 0.55 μM). Compound **5** showed moderate activity while compounds **4** and **6** displayed low cytotoxicity on all cell lines tested (Table 3) (Kuete and Efferth, 2015; Indrayanto et al., 2021). Comparing the activity of compounds **1** and **2** with those of **3**, **4** and **5** suggested that glucosylation at C-28 of compounds **1** and **2** was not favourable for the antiproliferative activity (Table 3). In addition, 6-methylation of the glucuronic acid of compound **5** was observed to enhance anticancer activities across the panel of cell lines used when compared with the activities of compound **4**.

Selectivity index (SI) was determined for the most active compounds, **3** and **5**, using the normal lung cell line (MRC5) (Table 4). SI, the ratio of toxicity to biological activity, is a measure of the differential toxicity of a chemical substance against cancerous cells in comparison to normal cells (Pritchett et al., 2014). A compound with SI value greater than 2 is generally considered selective for the cell line (Nogueira and do Rosário, 2010). SI values ranging from 0.44 to 1.15 were recorded for vincristine, the positive control. Previous works have also reported a lack of selectivity for vincristine (Rasli et al., 2023) and vinblastine (Segun et al., 2019). Compounds **3** and **5** were found to be more potently cytotoxic against the HeLa than the MCF-7 and Caco-2 cell lines (Table 3) and were also more selective than vincristine against the cancer cell lines compared to the normal lung cell line MRC5 (Table 4).

3. Conclusions

Three previously undescribed oleanane-type triterpene glycosides (**2, 3,** and **5**), two known triterpene glycosides (**1** and **4**), and one triterpene acid (**6**) have been isolated from the methanol root extract of *Olax subscorpioidea* Oliv. (Olacaceae), using several chromatographic techniques. Their chemical structures were established with extensive NMR analysis (1D and 2D) and MS experiments. Compounds **3** and **5** were found to be potently cytotoxic against the cervical cell line HeLa, with good selectivity index.

Table 3
Cytotoxic effects of compounds **1** to **6** on three human cancer cell lines and a non-cancerous cell line. Vincristine was used as a positive control. The data are presented as mean ± SEM (n = 3).

Compounds	IC_{50} ± SEM (μM)			
	HeLa	MCF-7	Caco-2	MRC5
1	>200	>200	>200	–
2	>200	>200	>200	–
3	7.42 ± 0.34	36.67 ± 1.23	35.83 ± 0.55	63.84 ± 1.06
4	67.58 ± 3.68	89.41 ± 1.91	50.9 ± 4.19	–
5	10.27 ± 1.26	43.83 ± 0.65	39.03 ± 4.38	67.0 ± 1.99
6	110.21 ± 15.64	66.63 ± 8.76	62.92 ± 0.82	–
Vincristine	1.42 ± 0.40	0.54 ± 0.06	1.33 ± 0.05	0.62 ± 0.01

Table 4
Selectivity index (SI) for compounds **3** and **5** and vincristine, when their cytotoxic potencies (IC_{50}) were compared in the HeLa, MCF-7 and Caco-2 cell lines versus the normal cell line MRC5.

Compounds	HeLa	MCF-7	Caco-2
1	–	–	–
2	–	–	–
3	8.60	1.74	1.78
4	–	–	–
5	6.52	1.53	1.72
6	–	–	–
Vincristine	0.44	1.15	0.47

4. Experimental

4.1. General methods

UV spectra were obtained on a UV–Visible spectrophotometer (Specord® 210, Analytik Jena, Germany). IR data were recorded on Cary 630 FTIR spectrophotometer (Agilent Technologies, USA). The melting point was obtained on Melting Point Apparatus (Griffin, UK). 1D and 2D NMR spectra were obtained on Bruker Avance III NMR spectrometer at 600 MHz (Massachusetts, U.S.A) for NMR experiments in methanol-d_4 using the solvent residue as internal standard. ^{1}H NMR experiment showed proton types; ^{13}C NMR showed carbon types; ^{13}C-DEPT-Q spectra were used to differentiate methyl, methylene, methine and quaternary carbons; ^{1}H–^{1}H COSY was used to determine correlations between neighbouring protons; ^{1}H–^{13}C HSQC revealed proton carbon connectivity over one bond; ^{1}H–^{13}C HMBC spectra helped in determining connectivities of protons to carbons over two or three bonds. All NMR data were processed using Bruker TopSpin 4.1.4. Chemical shifts were presented in part per million (ppm) and coupling constant (J values) were recorded in Hz. High-resolution mass spectrometric analyses (HR-ESI-MS) were recorded on 6530 Accurate-Mass Quadrupole Time-of-Flight (Q-TOF LC/MS) mass spectrometer (Agilent Technologies, USA). Rotary evaporator R-100 rotavapor (BUCHI, Switzerland) was used to concentrate the extract. Solid-phase extraction (SPE) was performed using a Strata C-18 cartridge (35 μm; 70 Å; 20 g, Phenomenex). Chromatographic separations were performed on Agilent 1260 Infinity HPLC system, and DIONEX Ultimate 3000 HPLC system (Thermo Fisher Scientific, Germany) connected with Phenomenex Luna® C_{18} column (150 × 21.2 mm, 10 μm). All solvents were of HPLC grade methanol, water (Fisher Chemical, Loughborough, United Kingdom), (Thermo Scientific, Germany). Cell culture materials include Dulbecco's Modified Eagle Medium (UK), Fetal bovine serum (Sigma-Aldrich, U.S.A), Gibco's trypLE Express (1X) (UK), Dulbecco's phosphate buffered-saline, MTT (3-(4,5-dimethylthiazol-2-yl)-2,5-diphenyl-2H-tetrazolium bromide) (Sigma-Aldrich, U.S.A), Tocris' vinblastine (Abingdon, UK), antibiotic-antimycotic (100X) (Gibco, U.S.A), L-glutamine 200 mM (100X) (Gibco, UK). MTT optical density values were measured on Tecan Spark 10M multimode microplate reader (Switzerland).

4.2. Plant material

The root bark of *Olax subscorpioidea* Oliv. (Olacaceae) was collected by Dr T. K. Odewo a taxonomist at Forestry Research Institute of Nigeria (FRIN), Ibadan, Nigeria, in November 2021. The herbarium specimen was deposited at Forest Herbarium Ibadan (FHI:113182) for authentication. The root material was washed, peeled, and air-dried under laboratory conditions. It was then ground into powder.

4.2.1. Extraction and isolation

The pulverized root (440 g), was extracted with methanol (MeOH) using the Soxhlet extraction procedure. The filtrate was then concentrated with rotary evaporator R-100 rotavapor (BUCHI, Switzerland) at about 40 °C. The extract was stored in an air-tight container before use. Before preparative HPLC analysis, the extract was fractionated by solid-phase extraction (SPE). The SPE cartridge (Strata C-18; 35 μm; 70 Å; 20 g) was conditioned by rinsing with MeOH (50 mL), followed by equilibrating with 100 mL of water. The extract (2 g) was dissolved in 40% MeOH in water, loaded on the cartridge and eluted with 20%, 50%, 80%, and 100% MeOH in water, and finally with 100% dichloromethane (200 mL each) (Sarker and Nahar, 2012) to afford five fractions, OSF1, OSF2, OSF3, OSF4, and OSF5, respectively. The fractions were concentrated by rotary evaporator, and consequently evaporated to dryness inside a fume hood. SPE fractions were screened against the human cervical cancer cell line (HeLa), colon cancer cell line (Caco-2) and breast cancer cell line (MCF-7). OSF3 showed cytotoxic effects on the tested cell lines. OSF3 (477 mg) was purified on reversed-phase preparative HPLC system with the mobile system: 70–90% MeOH-water containing 0.1% TFA, 30 min, brought to 100% MeOH, 5 min, maintained at 100% MeOH for another 5 min, then back to 70% MeOH in another 5 min, to afford OS1 (3.8 mg; t_R = 6.5 min); OS2 (14.8 mg; t_R = 9.5 min); OS3 (59.8 mg; t_R = 11.6 min); OS4 (79.7 mg; t_R = 13.1 min); OS5 (93.4 mg; t_R = 14.7 min); OS6 (2.8 mg; t_R = 18.1 min); OS7 (53.1 mg; t_R = 23.5 min); and OS8 (51.0 mg; t_R = 26.1 min). OS4 (79.7 mg) was re-purified on a reversed-phase semi-preparative HPLC system (Thermo Scientific UPLC 3000 Dionex) with mobile phase containing 0.1% TFA: 70–90% MeOH in water in 30 min to afford compound **1** (10 mg; t_R = 11.3 min) and compound **2** (5.8 mg; t_R = 12.7 min). OS7 (53.1 mg) was re-purified to isolate compound **3** (7.5 mg; t_R = 18.8 min). OS8 (51.0 mg) yielded compound **4** (1.5 mg; t_R = 20.5 min), **5** (3.8 mg; t_R = 22.7 min) and compound **6** (1.4 mg; t_R = 32.3 min). UV wavelengths were maintained at 220, 254, 280 & 310 nm.

4.2.2. Oleanolic acid 3-O-[α-L-rhamnopyranosyl-(1→3)-β-D-glucopyranosyl-(1 → 2)-6-O-methyl-β-D-glucuronopyranoside]-28-O-β-D-glucopyranosyl ester (2)

Amorphous, white powder; UV (MeOH) λ_{max} (log ε) 192.0 (−0.5636A) nm, 194.0 (−0.7342A) nm, 199.0 (−0.8431A) nm; IR (KBr) ν_{max} 3360 cm^{-1}, 2970 cm^{-1}, 1750 cm^{-1}, 1690 cm^{-1}, 1050 cm^{-1}; Melting point: 223–226 °C; ^1H and ^{13}C NMR data, see Tables 1 and 2; HR-ESI-MS *m/z* 1115.5630 $[M-H]^-$ and 1161.5706 $[M + HCOO]^-$ calculated for $C_{55}H_{88}O_{23}$ (calculated: 1115.5638).

4.2.3. Oleanolic acid 3-O-[β-D-glucopyranosyl-(1→4)-β-D-glucopyranosyl-(1 → 3)-β-D-glucopyranoside] (3)

Amorphous, white powder; UV (MeOH) λ_{max} (log ε) 193.0 (−0.0867A) nm, 199.0 (−0.3119A) nm, 206.0 (−1.5513A) nm; IR (KBr) ν_{max} 3300 cm^{-1}, 2930 cm^{-1}, 1750 cm^{-1}, 1690 cm^{-1}, 1020 cm^{-1}; Melting point: 265–267 °C; ^1H and ^{13}C NMR data, see Tables 1 and 2; HR-ESI-MS *m/z* 942.5188 $[M-H]^-$ calculated for $C_{48}H_{78}O_{18}$ (calculated: 942.5188).

4.2.4. Oleanolic acid 3-O-[β-D-glucopyranosyl-(1 → 4)-6-O-methyl-β-D-glucuronopyranoside] ester (5)

Amorphous, white powder; UV (MeOH) λ_{max} (log ε) 191.0 nm, 193.0 (−0.7542A) nm, 195.0 (−0.9086A) nm, 198.0 (8.0000A) nm, 200.0 (−0.2083A) nm; IR (KBr) ν_{max} 3350 cm^{-1}, 2920 cm^{-1}, 1750 cm^{-1}, 1695 cm^{-1}, 1020 cm^{-1}; Melting point: 238–240 °C; ^1H and ^{13}C NMR data, see Tables 1 and 2; HR-ESI-MS *m/z* 808.4537 $[M-H]^-$ calculated for $C_{43}H_{68}O_{14}$ (calculated: 808.4609).

4.3. Cell lines and cell culture

Human cancer cell lines: breast (MCF-7), colorectal (Caco-2), cervical (HeLa), and normal (non-cancerous) cell line MRC5 were originally obtained from the American Type Culture Collection (ATCC). The cell lines were grown in Dulbecco's Modified Eagle Medium (DMEM) supplemented with 10% foetal bovine serum (FBS), 1% 2 mM L-glutamine, and 1% penicillin-streptomycin solution, and kept in an incubator at 37 °C in a humidified atmosphere of 5% CO_2. They were passaged by removing the old medium, rinsing the cells with PBS (5 mL) and then adding 5 mL trypsin for about 60 s. Trypsin was removed and cells were incubated for about 5 min. The detached cells were flooded with the growth medium and triturated for a couple of minutes to get the cells into a homogeneous suspension. Cell density was determined using an automated plastic haemocytometer (C-Chip NanoEnTek, USA) and microscope-assisted counting. A volume of 100 μL, containing 7.5×10^3 cells, was added into each well of 96-well, flat bottom, μclear microtitre plates. Plates were then incubated for 24 h before experiments. Cells were visualised with an inverted microscope (Olympus CKX41, UK) at x10.

4.3.1. Cytotoxicity assay

The cytotoxic effect of isolated triterpenoid compounds from the root of *O. subscorpioidea* was measured by MTT colourimetric assay. Cell density optimisation (with 5×10^3 cells/well and 7.5×10^3 cells/well) revealed 7.5×10^3 cells/well to be optimal for cell growth for HeLa, MCF-7, Caco-2 and MRC5. After cells were cultured for 24 h, they were treated with SPE fractions (OSF1, OSF2, OSF3, OSF4 and OSF5). Working concentrations of 1, 10, 50, 100, 200 and 500 μg/mL for each sample were prepared from a 100 mg/mL stock solution in DMSO. All working dilutions were made using the full growth medium, with a final DMSO concentration of not more than 0.1% (Basar et al., 2015). The cells were treated with the dilutions, 100 μL/well, in triplicates. DMSO (at the %v/v in the highest sample concentration), growth medium, and vincristine were used as vehicle, negative and positive controls, respectively. The plates were incubated for 48 h. Then, 10 μL of 5 mg/mL MTT solution was added to all wells. The plates were incubated for 2 h to allow mitochondrial enzymatic action, converting the tetrazolium salt to formazan (Mosmann, 1983). The content of each well was then removed and 100 μL DMSO was added to solubilise the formed purple formazan (Aslantürk, 2018). The plates were gently shaken at 95 revolutions per minute for 5 min. The optical densities (OD) were read at 570 nm using Tecan Spark 30M multimode microplate reader (Switzerland). The above procedure was repeated for isolated compounds with the concentrations 12.5, 25, 50, 100, and 200 μM. The results were presented as concentrations of fractions or isolated compounds Each experiment was done in triplicate and repeated at least three independent times (n = 3).

Declaration of competing interest

The authors declare that they have no known competing financial interests or personal relationships that could have appeared to influence the work reported in this paper.

Data availability

Supplemental data will be made available on request

Acknowledgements

The authors thank the Commonwealth Scholarship Commission, United Kingdom for the award of the Commonwealth Split Site PhD Fellowship to Yemi Adekunle (NGCN-2021-184). Liverpool John Moores University, UK and University of Ibadan, Nigeria, are appreciated for their contributions toward Yemi's research. Lutfun Nahar gratefully acknowledges the financial support of the European Regional Development Fund - Project ENOCH (No. CZ.02.1.01/0.0/0.0/16_019/0000868) and the Czech Agency Grants - Project 23-05474S and Project 23-05389S.

Appendix A. Supplementary data

Supplementary data to this article can be found online at https://doi.org/10.1016/j.phytochem.2023.113853.

References

Adekunle, Y.A., Samuel, B.B., Akinleye, T.E., Adeniji, A.J., Ogbole, O.O., 2022a. Cytotoxicity analysis of nineteen medicinal plants extracts on breast adenocarcinoma (MCF-7) and rhabdomyosarcoma (RD) cancer cell lines. Trends Pharmaceut. Sci. 8 (1), 57–64. https://doi.org/10.30476/TIPS.2022.94313.1136.

Adekunle, Y.A., Samuel, B.B., Fatokun, A.A., Nahar, L., Sarker, S.D., 2022b. Olax subscorpioidea Oliv. (Olacaceae): an ethnomedicinal and pharmacological review. J. Nat. Prod. Discovery 1 (2), 1–15. https://doi.org/10.24377/jnpd.article673.

Agbabiaka, T.O., Adebayo, I.A., 2021. The medicinal properties of Olax subscorpioidea. In: Phytomedicine. Elsevier, pp. 555–580. https://doi.org/10.1016/b978-0-12-824109-7.00019-4.

Agrawal, P.K., Jain, D.C., 1992. 13C NMR spectroscopy of oleanane triterpenoids. Prog. Nucl. Magn. Reson. Spectrosc. 24 (1), 1–90. https://doi.org/10.1016/0079-6565(92)80011-4.

Ahmad, M.H., Jatau, A.I., Alshargi, O.Y., Julde, S.M., Mohammed, M., Muhammad, S., Mustapha, S., Bala, A.A., Wada, A.S., Aminu, M., Usman, A.M., 2021. Ethnopharmacological uses, phytochemistry, pharmacology, and toxicology of Olax subscorpioidea Oliv (Olacaceae): a review. Future J. Pharmaceut. Sci. 7 (1) https://doi.org/10.1186/s43094-021-00264-w.

Aliotta, G., de Napoli, L., Giordano, F., Piccialli, G., Piccialli, V., Santacroce, C., 1992. An oleanane triterpene from Anagallis arvensis. Phytochemistry 31 (3), 929–933. https://doi.org/10.1016/0031-9422(92)80041-C.

Aouane, C., Kabouche, A., Voutquenne-Nazabadioko, L., Sayagh, C., Martinez, A., Alabdul Magid, A., Kabouche, Z., 2022. Triterpenoid saponins from Anagallis monelli ssp. linifolia (L.) Maire and their chemotaxonomic significance. Phytochemistry 202, 113305. https://doi.org/10.1016/j.phytochem.2022.113305.

Aslantürk, Ö.S., 2018. In vitro cytotoxicity and cell viability assays: principles, advantages, and disadvantages. In: Genotoxicity-A Predictable Risk to Our Actual World, pp. 1–18. https://doi.org/10.5772/intechopen.71923.

Basar, N., Oridupa, O.A., Ritchie, K.J., Nahar, L., Osman, N.M.M., Stafford, A., Kushiev, H., Kan, A., Sarker, S.D., 2015. Comparative cytotoxicity of Glycyrrhiza glabra roots from different geographical origins against immortal human keratinocyte (HaCaT), lung adenocarcinoma (A549) and liver carcinoma (HepG2) cells. Phytother Res. 29 (M), 944–948. https://doi.org/10.1002/ptr.5329.

de Bruyn, A., Anteunis, M., de Gussem, R., Dutton, G.G.S., 1976. 1H-N.m.r. study of l-rhamnose, methyl α-l-rhamnopyranoside, and 4-O-β-d-galactopyranosyl-l-rhamnose in deuterium oxide. Carbohydr. Res. 47 (1), 158–163. https://doi.org/10.1016/S0008-6215(00)83559-4.

Delaude, C., Huls, R., 1982. Contribution à l'étude phytochimique des Olacaceae. Analyse de la saponine d'Olax obtusifolia De Wild. Bull. Soc. R. Sci. Liege 51 (1–2), 47–50.

Do, V.M., Tran, C.L., Nguyen, T.P., 2020. Polysciosides J and K, two new oleanane-type triterpenoid saponins from the leaves of Polyscias fruticosa (L.) harms. cultivating in an Giang Province, Viet Nam. Nat. Prod. Res. 34 (9), 1250–1255. https://doi.org/10.1080/14786419.2018.1557657.

Feng, J.-H., Chen, W., Zhao, Y., Ju, X.-L., 2009. Anti-tumor activity of oleanolic, ursolic and glycyrrhetinic acid. Open Nat. Prod. J. 2 (1), 48–52. https://doi.org/10.2174/1874848100902010048.

Ferlay, J., Colombet, M., Soerjomataram, I., Parkin, D.M., Piñeros, M., Znaor, A., Bray, F., 2021. Cancer statistics for the year 2020: an overview. Int. J. Cancer 149 (4), 778–789. https://doi.org/10.1002/ijc.33588.

Forgacs, P., Provost, J., 1981. Olaxoside, a saponin from Olax andronensis, Olax glabriflora and Olax psittacorum. Phytochemistry 20 (7), 1689–1691. https://doi.org/10.1016/S0031-9422(00)98556-X.

Gaglianone, M., Laugieri, M.E., Rojas, A.L., Coppola, M.R., Piacente, F., Fiori, P.L., Tonetti, M.G., 2022. The L-rhamnose biosynthetic pathway in trichomonas vaginalis: identification and characterization of UDP-D-glucose 4,6-dehydratase. Int. J. Mol. Sci. 23, 14587 https://doi.org/10.3390/ijms232314587.

Gao, L., Zhang, L., Wang, L.M., Liu, J.Y., Cai, P.L., Yang, S.L., 2012. New triterpenoid saponins from Patrinia scabiosifolia. J. Asian Nat. Prod. Res. 14 (4), 333–341. https://doi.org/10.1080/10286020.2011.653685.

Gbadamosi, I.T., Erinoso, S.M., 2016. A review of twenty ethnobotanicals used in the management of breast cancer in Abeokuta, Ogun State, Nigeria. African J. Pharm. Pharmacol. 10 (27), 546–564. https://doi.org/10.5897/ajpp2015.4327.

Giner, J.L., Feng, J., Kiemle, D.J., 2016. NMR tube degradation method for sugar analysis of glycosides. J. Nat. Prod. 79 (9), 2413–2417. https://doi.org/10.1021/acs.jnatprod.6b00180.

Gyanani, V., Haley, J.C., Goswami, R., 2021. Challenges of current anticancer treatment approaches with focus on liposomal drug delivery systems. Pharmaceuticals 14 (835), 1–27. https://doi.org/10.3390/ph14090835.

Huan, V.D., Yamamura, S., Ohtani, K., Kasai, R., Yamasaki, K., Nham, N.T., Chau, H.M., 1998. Oleanane saponins from Polyscias fruticosa. Phytochemistry 47 (3), 451–457. https://doi.org/10.1016/S0031-9422(97)00618-3.

Indrayanto, G., Putra, G.S., Suhud, F., 2021. Validation of in-vitro bioassay methods: application in herbal drug research. In: Profiles of Drug Substances, Excipients and Related Methodology, first ed., Vol. 46. Elsevier Inc. https://doi.org/10.1016/bs.podrm.2020.07.005.

Jiang, N., Dillon, F.M., Silva, A., Gomez-Cano, L., Grotewold, E., 2021. Rhamnose in plants - from biosynthesis to diverse functions. Plant Sci. 302, 110687 https://doi.org/10.1016/j.plantsci.2020.110687.

Kamsteeg, J., Brederode, J. Van, Nigtevecht, G. Van, 1978. The formation of UDP-L-rhamnose from UDP-D-glucose by an enzyme preparation of red campion (Silene Dioica (L) clairv) leaves. FEBS (Fed. Eur. Biochem. Soc.) Lett. 91 (2), 281–284. https://doi.org/10.1016/0014-5793(78)81192-2.

Kuete, V., Efferth, T., 2015. African flora has the potential to fight multidrug resistance of cancer. BioMed Res. Int. https://doi.org/10.1155/2015/914813, 2015.

Li, S., Chen, F., Li, Y., Wang, L., Li, H., Gu, G., Li, E., 2022. Rhamnose-containing compounds: biosynthesis and applications. Molecules 27 (16), 5315. https://doi.org/10.3390/molecules27165315.

Liang, D., Hao, Z.-Y., Zhang, G.-J., Zhang, Q.-J., Chen, R.-Y., Yu, D.-Q., 2011. Cytotoxic triterpenoid saponins from Lysimachia clethroides. J. Nat. Prod. 74, 2128–2136. https://doi.org/10.1021/np2004038.

Mahato, S.B., Kundu, A.P., 1994. 13C nmr spectra of pentacyclic triterpenoids-a and some salient features. Phytochemistry 37 (6), 1517–1575.

Mosmann, T., 1983. Rapid colorimetric assay for cellular growth and survival: application to proliferation and cytotoxicity assays. J. Immunol. Methods 65, 55–63. https://doi.org/10.1039/c6ra17788c.

Nga Thi, V., Minh Suong, H.T., My Huong, N.T., Huy, D.T., Phi Phung, N.K., 2019. Triterpenoid glycosides from olax imbricata. Sci. Technol. Dev. J. 22 (3), 324–334. https://doi.org/10.32508/stdj.v22i3.1660.

Nogueira, F., do Rosário, V.E., 2010. Epidemiology of Saint Louis encephalitis virus in the Brazilian Amazon region and in the State of Mato Grosso do Sul, Brazil: elevated prevalence of antibodies in horses. Revista Pan-Amazônica de Saúde 1 (3), 109–124. https://doi.org/10.5123/s2176-62232010000100012.

Odoma, S., Umar Zezi, A., Mohammed Danjuma, N., Ahmed, A., Garba Magaji, M., 2017. Elucidation of the possible mechanism of analgesic actions of butanol leaf fraction of Olax subscorpioidea Oliv. J. Ethnopharmacol. 199, 323–327. https://doi.org/10.1016/j.jep.2016.12.052.

Odoma, S., Zezi, A.U., Danjuma, M.N., Abubakar, A., Magaji, G.M., 2020. Effects of aqueous and butanol leaf fractions of olax subscorpioidea oliv. On inflammatory cytokines in wistar rats. Tropical Journal of Natural Product Research 4 (9), 606–611. https://doi.org/10.26538/tjnpr/v4i9.19.

Parikh, N.R., Mandal, A., Bhatia, D., Siveen, K.S., Sethi, G., Bishayee, A., 2014. Oleanane triterpenoids in the prevention and therapy of breast cancer: current evidence and future perspectives. Phytochemistry Rev. 13 (4), 793–810. https://doi.org/10.1007/s11101-014-9337-5.

Patkhullaeva, M., Mzhel'skaya, L.C., Abubakirov, N.K., 1972. Triterpene glycosides of Ladyginia bucharica II. The structure of Ladyginosides A and B. Khimia Priroduykh Soedinenii 8, 466.

Pertuit, D., Mitaine-Offer, A.C., Miyamoto, T., Tanaka, C., Delaude, C., Lacaille-Dubois, M.A., 2018. Triterpene saponins of the root bark of Olax obtusifolia De Wild. Phytochem. Lett. 28 (September), 174–178. https://doi.org/10.1016/j.phytol.2018.09.018.

Pritchett, J.C., Naesens, L., Montoya, J., 2014. Treating HHV-6 infections: the laboratory efficacy and clinical use of anti-HHV-6 agents. In: Flamand, L., Lautenschlager, I., Krueger, G. (Eds.), *Human Herpesviruses HHV-6A, HHV-6B, and HHV-7* (Third Edit). Elsevier B.V. https://doi.org/10.1016/B978-0-444-62703-2.00019-7.

Rasli, N.R., Hamid, A., Awang, N., Kamaludin, N.F., 2023. Series of organotin(IV) compounds with different dithiocarbamate ligands induced cytotoxicity, apoptosis and cell cycle arrest on Jurkat E6.1, T acute lymphoblastic leukemia cells. Molecules 28 (3376), 1–14. https://doi.org/10.3390/molecules28083376.

ReFaey, K., Tripathi, S., Grewal, S.S., Bhargav, A.G., Quinones, D.J., Chaichana, K.L., Antwi, S.O., Cooper, L.T., Meyer, F.B., Dronca, R.S., Diasio, R.B., Quinones-Hinojosa, A., 2021. Cancer mortality rates increasing vs cardiovascular disease mortality decreasing in the world: future implications. Mayo Clin. Proc.: Innovat. Qual. Outcomes 5 (3), 645–653. https://doi.org/10.1016/j.mayocpiqo.2021.05.005.

Sarker, S.D., Nahar, L., 2012. Natural products isolation: methods and protocols. In: Methods in Molecular Biology, third ed., Vol. 864. Springer Science+Business Media, LLC. https://doi.org/10.1007/978-1-61779-624-1_1.

Seebacher, W., Simic, N., Weis, R., Saf, R., Kunert, O., 2003. Complete assignments of 1H and 13C NMR resonances of oleanolic acid, 18α-oleanolic acid, ursolic acid and their 11-oxo derivatives. Magn. Reson. Chem. 41 (8), 636–638. https://doi.org/10.1002/mrc.1214.

Segun, P.A., Ogbole, O.O., Ajaiyeoba, E.O., 2018. Medicinal plants used in the management of cancer among the ijebus of southwestern Nigeria. J. Herb. Med. 14, 68–75. https://doi.org/10.1016/j.hermed.2018.04.002.

Segun, P.A., Ogbole, O.O., Ismail, F.M.D., Nahar, L., Evans, A.R., Ajaiyeoba, E.O., Sarker, S.D., 2019. Bioassay-guided isolation and structure elucidation of cytotoxic stilbenes and flavonols from the leaves of Macaranga barteri. Fitoterapia 134, 151–157. https://doi.org/10.1016/j.fitote.2019.02.019, 2019.

Soladoye, M.O., Amusa, N.A., Raji-Esan, S.O., Chukwuma, E.C., Taiwo, A.A., 2010. Ethnobotanical survey of anti-cancer plants in Ogun State, Nigeria. Ann. Biol. Res. 1 (4), 261–273.

Song, H., Rogers, N.J., Allison, S.J., Brabec, V., Bridgewater, H., Kostrhunova, H., Markova, L., Phillips, R.M., Pinder, E.C., Shepherd, S.L., Young, L.S., Zajac, J., Scott, P., 2019. Discovery of selective, antimetastatic and anti-cancer stem cell metallohelices: via post-assembly modification. Chem. Sci. 10 (37), 8547–8557. https://doi.org/10.1039/c9sc02651g.

Stefaniak, M., Łopatkiewicz, G., Antkowiak, M., Mlynarski, J., 2018. Stereocontrolled synthesis of oleanolic saponin ladyginoside A isolated from Ladyginia bucharica. Carbohydr. Res. 458–459, 35–43. https://doi.org/10.1016/j.carres.2018.01.011.

Stewart, B.W., Wild, C.P., 2014. World cancer report 2014. In: World Health Organization. WHO) Press, Lyon.

Sule, M.I., Hassan, H., Pateh, U., Ambi, A., 2011. Triterpenoids from the leaves of olax mannii. Nigerian J. Basic Appl. Sci. 19 (2), 193–196. http://www.ajol.info/index.php/njbas/index.

Sung, H., Ferlay, J., Siegel, R.L., Laversanne, M., Soerjomataram, I., Jemal, A., Bray, F., 2021. Global cancer statistics 2020: GLOBOCAN estimates of incidence and mortality worldwide for 36 cancers in 185 countries. CA A Cancer J. Clin. 71 (3), 209–249. https://doi.org/10.3322/caac.21660.

Tsakem, B., Ponou, K.B., Toussie, B.T., Tematio, R.F., Noundou, X.S., Krause, R.W.M., Teponno, R.B., Tapondjou, L.A., 2022. Natural products chemistry of botanical medicines from Cameroonian plants. In: Siwe-Noundou, X., Cooper, R. (Eds.), Natural Products Chemistry of Global Plants, First Edit). Taylor & Francis Group CRS Press. https://doi.org/10.1201/9780429506734.

Ukwe, V.C., Ubaka, M.C., Madusque, J.U., 2010. Evaluation of the antiulcer activity of Olax subscorpioidea Oliv. roots in rats. Asian Pac. J. Tropical Med. 3 (1), 13–16. https://doi.org/10.1016/S1995-7645(10)60022-3.

Zheng, Q., Koike, K., Han, L.K., Okuda, H., Nikaido, T., 2004. New biologically active triterpenoid saponins from scabiosa tschiliensis. J. Nat. Prod. 67 (4), 604–613. https://doi.org/10.1021/np0304722.